

This is a copy of the published version, or version of record, available on the publisher's website. This version does not track changes, errata, or withdrawals on the publisher's site.

High-pressure neutron diffraction study of magnetite, Fe₃O₄, nanoparticles

Lei Tan, Andrei V. Sapelkin, Alston J. Misquitta, Craig L. Bull, He Lin, Haolai Tian, Haijun Huang, and Martin T. Dove

Published version information

Citation: L Tan et al. High-pressure neutron diffraction study of magnetite, Fe₃O₄, nanoparticles. Appl Phys Lett 120, no. 23 (2022): 233101.

DOI: [10.1063/5.0085164](https://doi.org/10.1063/5.0085164)

This article may be downloaded for personal use only. Any other use requires prior permission of the author and AIP Publishing. This article appeared as cited above.

This version is made available in accordance with publisher policies. Please cite only the published version using the reference above. This is the citation assigned by the publisher at the time of issuing the APV. Please check the publisher's website for any updates.

This item was retrieved from **ePubs**, the Open Access archive of the Science and Technology Facilities Council, UK. Please contact epublications@stfc.ac.uk or go to <http://epubs.stfc.ac.uk/> for further information and policies.

High-pressure neutron diffraction study of magnetite, Fe_3O_4 , nanoparticles

Cite as: Appl. Phys. Lett. **120**, 233101 (2022); <https://doi.org/10.1063/5.0085164>
 Submitted: 13 January 2022 • Accepted: 15 May 2022 • Published Online: 06 June 2022

 Lei Tan,  Andrei V. Sapelkin,  Alston J. Misquitta, et al.



View Online



Export Citation



CrossMark

ARTICLES YOU MAY BE INTERESTED IN

[Mapping electric fields in real nanodevices by operando electron holography](#)
 Applied Physics Letters **120**, 233501 (2022); <https://doi.org/10.1063/5.0092019>

[Electron transport properties of a narrow-bandgap semiconductor \$\text{Bi}_2\text{O}_2\text{Te}\$ nanosheet](#)
 Applied Physics Letters **120**, 233102 (2022); <https://doi.org/10.1063/5.0092046>

[40 GHz waveguide-integrated two-dimensional palladium diselenide photodetectors](#)
 Applied Physics Letters **120**, 231102 (2022); <https://doi.org/10.1063/5.0091625>



1 qubit

Shorten Setup Time
Auto-Calibration
More Qubits

Fully-integrated
Quantum Control Stacks
Ultrastable DC to 18.5 GHz
 Synchronized <<1 ns
 Ultralow noise



100s qubits

[visit our website >](#)



High-pressure neutron diffraction study of magnetite, Fe_3O_4 , nanoparticles

Cite as: Appl. Phys. Lett. **120**, 233101 (2022); doi: [10.1063/5.0085164](https://doi.org/10.1063/5.0085164)

Submitted: 13 January 2022 · Accepted: 15 May 2022 ·

Published Online: 6 June 2022



View Online



Export Citation



CrossMark

Lei Tan,^{1,2}  Andrei V. Sapelkin,²  Alston J. Misquitta,²  Craig L. Bull,^{3,4}  He Lin,⁵  Haolai Tian,^{6,7} 
Haijun Huang,¹  and Martin T. Dove^{1,2,8,9,a)} 

AFFILIATIONS

¹Department of Physics, School of Sciences, Wuhan University of Technology, 205 Luoshi Road, Hongshan district, Wuhan, Hubei 430070, China

²School of Physical and Chemical Sciences, Queen Mary University of London, Mile End Road, London E1 4NS, United Kingdom

³ISIS Facility, Rutherford Appleton Laboratory, Harwell Campus, Didcot, Oxfordshire OX11 0QX, United Kingdom

⁴EaStCHEM School of Chemistry, University of Edinburgh, Joseph Black Building, Edinburgh EH9 3FJ, United Kingdom

⁵Shanghai Synchrotron Radiation Facility, Shanghai Advanced Research Institute, Chinese Academy of Sciences, 99 Haikue Road, Shanghai 201210, China

⁶Spallation Neutron Source Science Center, Dongguan, Guangdong 523803, China

⁷Institute of High Energy Physics, Chinese Academy of Sciences, Beijing 100049, China

⁸College of Computer Science, Sichuan University, No. 24 South Section 1, Yihuan Road, Chengdu, Sichuan 610065, China

⁹School of Mechanical Engineering, Dongguan University of Technology, Songshan Lake, Dongguan, Guangdong 523000, China

^{a)} Author to whom correspondence should be addressed: martin.dove@icloud.com

ABSTRACT

We use *in situ* high-pressure neutron powder diffraction to study elastic properties of Fe_3O_4 magnetite nanoparticles of different sizes. It is found that nanoparticles are elastically softer than the bulk. Apart from the smallest nanoparticle of diameter 8 nm, the atomic and magnetic structures do not change significantly with nanoparticle size or pressure. The 8 nm sample appears to take a disordered spinel structure instead of the inverse spinel structure of the bulk and larger nanoparticles, as seen in bond lengths and magnetic structures. Synchrotron x-ray total scattering was used to support this interpretation. Furthermore, this study suggests that the influence of magnetic disorder at the nanoparticle surface is significant for the size of 8 nm.

Published under an exclusive license by AIP Publishing. <https://doi.org/10.1063/5.0085164>

Magnetite (Fe_3O_4) is one of the oldest known materials and has proven to be an important high-temperature ferrimagnet. Because of this, its magnetic and crystal structures have been extensively studied.^{1–6} Nanoparticles of magnetite have found applications in catalysis,⁷ electronic devices,^{8,9} and information storage.¹⁰ Although the structures and properties of magnetite nanoparticles have been studied using several different approaches,^{11–13} including x-ray diffraction (XRD) and polarized small-angle neutron scattering,^{14–16} there are fewer studies regarding the effects of pressure on magnetite nanoparticles than on the bulk.

The research of magnetite nanoparticles under pressure is mainly focused on the change of magnetic property^{11,17} and structural transition.¹² Indeed, there are research works about the elastic properties of Fe_3O_4 nanoparticles at a single size under high pressure.¹³ However, as

far as we are concerned, there are no reported studies of the compressibility of different sizes of magnetite nanoparticles under pressure.

Because of the high surface-to-volume ratio of nanoparticles, nanoparticles may show different behaviors under pressure than their bulk crystalline counterparts, and in ways that are not always easy to understand. For example, nanoparticles of $\gamma\text{-Fe}_2\text{O}_3$ (maghemite),¹⁸ Ge_3N_4 ,¹⁹ Au,^{20,21} and Ag²¹ show an increase in compressibility for smaller particle size, whereas Pd,²² CdSe,²³ ZnS,²⁴ Pt,²⁵ ZnFe_2O_4 ,²⁶ and TiO_2 ²⁷ show the opposite. This diversity of behavior is not understood.

In this paper, we study the effects of pressure on magnetite nanoparticles of different sizes, down to 8 nm, using neutron powder diffraction. This gives us a good opportunity to study the size-dependence of elasticity at the nanoscale in a systematic way.

Furthermore, by using neutron diffraction, we are able to understand how pressure affects the magnetic structure of magnetite nanoparticles.

We prepared three different sizes of Fe_3O_4 nanoparticles for the high-pressure neutron powder diffraction experiment. Details of the synthesis method are described in Sec. S1 of the [supplementary material](#). The samples were all characterized with x-ray diffraction (XRD) measurements (Fig. S1 in the [supplementary material](#)) to ensure there is no impurity phase. As expected, the peaks for smaller nanoparticles are broader, and from the widths of the peaks, we deduced sample sizes of 25 ± 3 , 15 ± 2 , and 8 ± 2 nm using the Scherrer equation.³⁰

The neutron powder diffraction data were collected at the PEARL diffractometer of the UK spallation source ISIS at the Rutherford Appleton Laboratory.³¹ Pressure to the sample was applied using a Paris–Edinburgh press, which uses opposed zirconia-toughened alumina (ZTA) anvils. The sample is contained within a gasket, which contained a small amount of lead to act as the calibration of pressure. Thus, in the structure refinement of data analysis, there are zirconia and aluminum phases from the anvil and the lead phase from the pressure marker. Each sample was mixed with a deuterated ethanol–methanol (4:1 by volume) mixture to act as the pressure-transmission medium. Measurements were performed over the pressure range 0–5.9 GPa at ambient temperatures.

We show the neutron diffraction patterns of Fe_3O_4 nanoparticles and the bulk phase in the [supplementary material](#), Figs. S2 and S3. Under the applied pressure, the Bragg diffraction peaks, highlighted in Fig. S2, shift to lower d values, indicating the compression of the lattice. Rietveld refinements were used in the refinement of the atomic and magnetic structures. For reference, the crystal structure of magnetite is shown in [Fig. 1](#). The magnetic structure has an antiparallel arrangement of spins in the tetrahedral and octahedral sites, giving a magnetic space group of $R3m'$. The details of Rietveld refinements and an example of the fitting are shown in Sec. S3 of the [supplementary material](#).

It is found that the value of the lattice parameter of Fe_3O_4 becomes smaller with decreasing particle size as shown in [Fig. 2](#) and

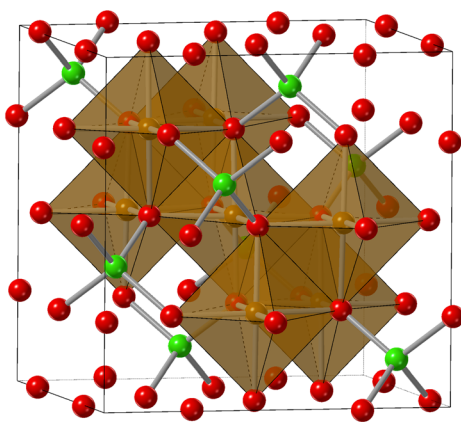


FIG. 1. The crystal structure of Fe_3O_4 in the inverse spinel structure, space group $Fd\bar{3}m$.^{28,29} Oxygen atoms are shown as red spheres. The tetrahedral Fe^{3+} sites are shown as green spheres with bonds to connected oxygen atoms to highlight the coordination. The octahedral sites containing a disordered arrangement of Fe^{2+} and Fe^{3+} atoms are shown as brown translucent polyhedra.

[Fig. S7](#) from the [supplementary material](#). The results for the bulk are in reasonable agreement with the previous data reported by Klotz *et al.*³² with small differences lying within the error bars, indicating the robustness of our experimental results. While the lattice parameters of metal nanoparticles generally decrease with smaller size,³³ for many oxides, the opposite behavior can be found.³⁴ One example is that of CeO_2 nanoparticles,^{35,36} which shows an obvious lattice expansion in nanoparticles compared with its bulk counterparts. Diehm *et al.*,³⁴ who have summarized extensive experiment data and theoretic calculation, highlighted the crucial role played by the surface stress³⁷ in the difference between expansion and contraction of lattices with decreasing particle size. With decreasing size, the surface to volume ratio increases, and the effect of surface stress becomes more pronounced. Thus, negative surface stresses would lead to negative capillary pressure, δp ,³⁸ resulting in lattice expansion. However, our magnetite nanoparticles show an opposite result that the lattice shrinks with decreasing particle size, which implies that there is a possibility that there is no significant surface stress in our system.

The third order Birch–Murnaghan equation of states is given as below, which was applied to determine the bulk modulus B and its first pressure derivative B' ,

$$P(V) = \frac{3B_0}{2} \left[\left(\frac{V_0}{V} \right)^{\frac{2}{3}} - \left(\frac{V_0}{V} \right)^{\frac{5}{3}} \right] \times \left\{ 1 + \frac{3}{4}(B' - 4) \left[\left(\frac{V_0}{V} \right)^{\frac{2}{3}} - 1 \right] \right\},$$

where P and V are the applied pressure and the volume of unit cell, respectively, V_0 and B_0 are the volume and bulk modulus, respectively, at $P = 0$, and B' is the derivative of the bulk modulus, dB/dP , at $P = 0$. The second order equation is equivalent to the case $B' = 4$. Both second and third order equations were fitted to the data as shown in [Fig. 2](#), and the results for B_0 and B' are listed in [Table I](#). Ferrari *et al.* reported that the bulk modulus of the Fe_3O_4 nanoparticle with a grain size of 55(9) nm is 152(9) GPa after fitting with a third order

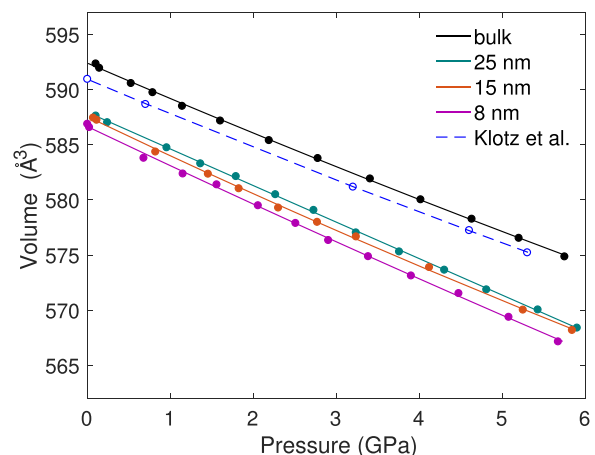


FIG. 2. Results from fitting the pressure-dependence of volume with the Birch–Murnaghan equation of the magnetite bulk phase and the three different size nanoparticles. The blue open circles and dashed line represent the neutron diffraction results of the magnetite bulk phase reported by Klotz *et al.*³²

Birch–Murnaghan equation; this value is lower than our results shown in Table I, but differences are only three times the stated error and may be considered to be consistent with the data of this study. The fitted values of the bulk modulus for both second and third order equations are 181(1) GPa, which is in reasonable agreement with the value of 186(5) GPa obtained from the previous neutron diffraction study.³⁹

As shown in Table I, the bulk modulus of three different sizes of nanoparticles behaves very differently from the bulk sample. Both show that the bulk modulus B_0 is reduced as the nanoparticle size is reduced with a reduction of 12%–15%. We noted in the introduction that some nanoparticles become softer and some become harder compared to the bulk. Rodenbough *et al.*³⁵ and Bian *et al.*⁴⁰ reported a variation of the bulk modulus in CeO₂ and PbS nanoparticles, showing a maximum in the value of the bulk modulus with particle size. Although these maxima actually occur in the gap in our data between the bulk and first point—the nanoparticles in our study here are smaller than in most other studies—our data show no evidence for such a maximum. What is clear from our results is that Fe₃O₄ nanoparticles become softer with decreasing size. Ferrari *et al.* observed the same decrease in the bulk modulus of Fe₃O₄ and ZnFe₂O₄ nanoparticles with a spinel structure.

Figure 3 shows the variation with pressure of the oxygen x coordinate [Fig. 3(a)], tetrahedral Fe–O distance [Fig. 3(b)], and octahedral

Fe–O distance [Fig. 3(c)] for the different samples. Note that for the oxygen fractional coordinate of the form (x, x, x) , the tetrahedral and octahedral bond lengths are $\sqrt{3}a(x - 1/8)$ and $a(1/2 - x)$, respectively. The x coordinate of the oxygen atom in the bulk and the nanoparticle phases appears to be virtually independent of pressure. This means that most of the variations of the two bond lengths with pressure are driven by the variation in the lattice parameter with both bond lengths changing in equal proportion. Rozenberg *et al.*⁴ reported similar results that the pressure dependency of x is small over the 0–7 GPa range for bulk magnetite. It is noted that the oxygen coordinate of magnetite bulk is around 0.253 with increasing pressure, which is consistent with the value of the oxygen coordinate reported by Klotz *et al.*³²

The oxygen coordinate and, hence, the two bond lengths do not show a systematic variation with nanoparticle size. It is known that with the decrease in particle size, the relatively large surface to volume ratio means that the surface atoms play a crucial role in determining the average structure, leading to different effective bond lengths.⁴⁰ We have plotted the bond length in the tetrahedral site against that of the octahedral site (see Fig. S9 in the supplementary material). The interesting fact is that with decreasing size, the tetrahedral Fe–O distances increase, in contrast to the decrease in the octahedral Fe–O distance. This opposite variation tendency of the bond lengths in the two sites

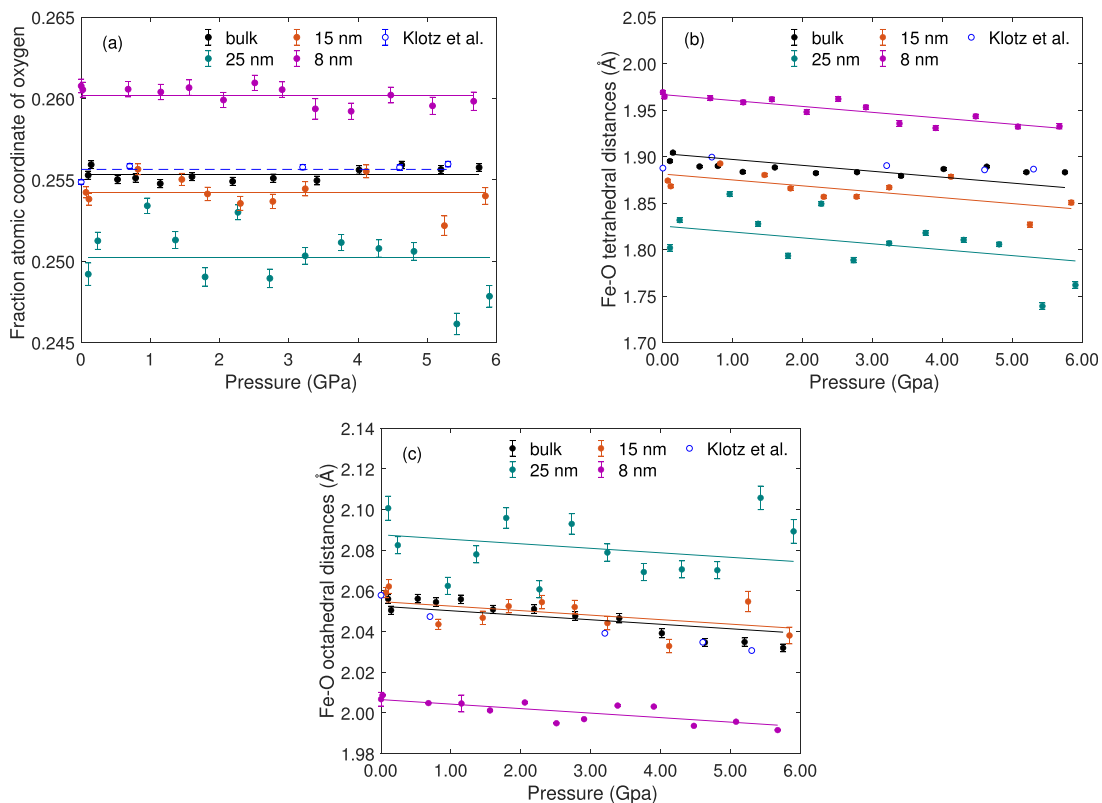


FIG. 3. (a) The fractional atomic coordinate of oxygen as a function of pressure for Fe₃O₄ bulk and nanoparticles of size 25, 15, and 8 nm. The fitted straight lines are guide to the eye for each dataset. The blue open circles and dashed line are for the neutron diffraction results on the bulk phase of Fe₃O₄ reported by Klotz *et al.*³² (b) and (c) Corresponding changes in the tetrahedral and octahedral Fe–O bond lengths, respectively. (a) Fractional atomic coordinate x , (b) tetrahedral bond length, and (c) octahedral bond length.

TABLE I. Results from fitting the data to second and third order Birch–Murnaghan equations. The study of bulk Fe_3O_4 ³⁹ and another independent study of a Fe_3O_4 nanoparticle of diameter 55(9) nm (Ref. 13) are also shown in the table for comparison.

Size (nm)	Lattice parameter, a'' (Å)	V_0 (Å ³)	B_0 (GPa) (second-order)	B_0 (GPa) (third-order)	B'
Bulk	8.3984(1)	592.36(2)	181(1)	182(5)	4(2)
Bulk ³⁹	8.392(3)	591(1)	186(5)	183(5)	...
55(9)	8.39(1)	590(2)	...	152(9)	5.2 (1.3)
25(3)	8.3760(4)	587.63(2)	163(2)	176(4)	−0.4(9)
15(2)	8.3752(4)	587.46(3)	164(1)	163(7)	4.5(9)
8(2)	8.3725(1)	586.90(2)	159(2)	164(6)	2.1(9)

may support this idea that the particle size did play an important role in the average structure, which caused the different bond lengths for the nanoparticles with different sizes.

However, there is a significant difference between the bigger size samples and the 8 nm sample, where there is a sudden increase in the value of x , leading to a lengthening of the tetrahedral Fe–O bond length and corresponding shortening of the octahedral Fe–O bond length. We consider three possibilities for the striking difference of the 8 nm sample compared with other sizes, namely, the 8 nm nanoparticle has the maghemite structure, it has the normal spinel structure with Fe^{2+} on the tetrahedral site, and there is complete electronic disorder.

In order to test the three possible alternative structures, we have performed a synchrotron x-ray total scattering measurement of the 8 nm nanoparticle sample at ambient pressure. The technique of “total scattering” measured a precise and complete scattering pattern of samples over a wide range of scattering vectors. After Fourier transformation of total scattering data, we obtain the pair distribution function (PDF) in real space. The equations and details about the principles of PDF are discussed in Sec. S4 of the [supplementary material](#). In the analysis of the structure, we have performed calculations of the PDFs using a special module within the General Utility Lattice Program (GULP) to give a noise-free simulated PDF as a comparison. The first possibility might be that the 8 nm sample has the maghemite structure, which has only Fe^{3+} cations and oxygen vacancies with the composition as $(\text{Fe}^{3+})[\text{Fe}^{3+}_{5/6}\square_{1/6}]_2\text{O}_4$ (where “ \square ” means a vacancy, “()” means the tetrahedral site, and “[]” means the octahedral site). Effectively, the atomic structures of magnetite and maghemite give almost identical calculations of the PDF (shown in Fig. S8 in the [supplementary material](#)). Aside from that Rietveld refinements give the same longer Fe–O bond lengths, which are inconsistent with both magnetite and maghemite structures. Thus, the possibility of the maghemite structure is excluded.

The second possibility is that the structure of the 8 nm sample has changed to the normal spinel structure with Fe^{2+} cations on the tetrahedral sites and all Fe^{3+} cations on the octahedral sites. Fe^{2+} and Fe^{3+} adopt bond lengths of 1.990 and 2.016 Å in tetrahedral and octahedral coordinations, respectively.⁴¹ This suggestion is consistent with the bond lengths observed in Figs. 3(b) and 3(c). The measured PDF for the 8 nm sample is compared to calculations of the PDF for the ordered normal spinel in Fig. 4. We can see that the PDF calculated for the normal spinel agrees with the experimental PDF in the long range $r > 8$ Å). However, in the short range $r < 6$ Å), which contains the information of the local structure, the normal spinel model gives an extra peak around

2.2 Å. Therefore, the structure of the 8 nm sample is neither a normal spinel nor an inverse spinel structure, but appears to be intermediate to these two states. Based on this idea, we have considered a disordered spinel structure, which is our third model. The calculated PDF of this model is shown in Fig. 4 with blue lines. It can be seen that the extra peak is not reproduced in the disordered model. Overall, the PDF calculated from the disordered spinel model agrees best with the experimental PDF. It also supports the bond length of a general spinel structure but with a disordered spinel instead of an ordered normal spinel structure.

For the change of the magnetic structure with pressure, we have plotted the variation of the refined values of magnetic moments with pressure for the tetrahedral [Fig. 5(a)] and octahedral [Fig. 5(b)] cation sites, respectively, for the bulk and nanoparticle phases. The magnetic moments in all the samples do not show any significant variation with pressure, consistent with previous suggestions that the spin state of iron in magnetite remains stable until higher pressures than 6.5 GPa.⁴² Moreover, the value of the magnetic moment in the bulk sample is consistent with previous data.³²

The magnetic moment of the 8 nm nanoparticle shows a significant difference compared with the other sizes and the bulk, which is

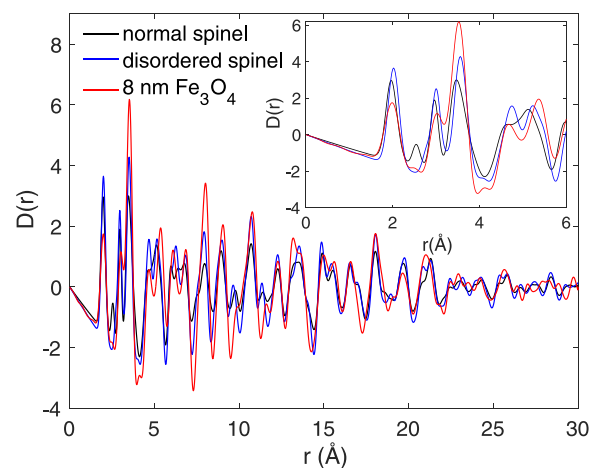


FIG. 4. The simulated PDFs of the ordered normal spinel structure (black line) and the disordered normal spinel structure (blue line), compared with the PDF measured in the Shanghai synchrotron source. The inset graph is magnifications of the range from 0 to 6 Å to indicate the local structure difference between the ordered spinel structure and the disordered structure.

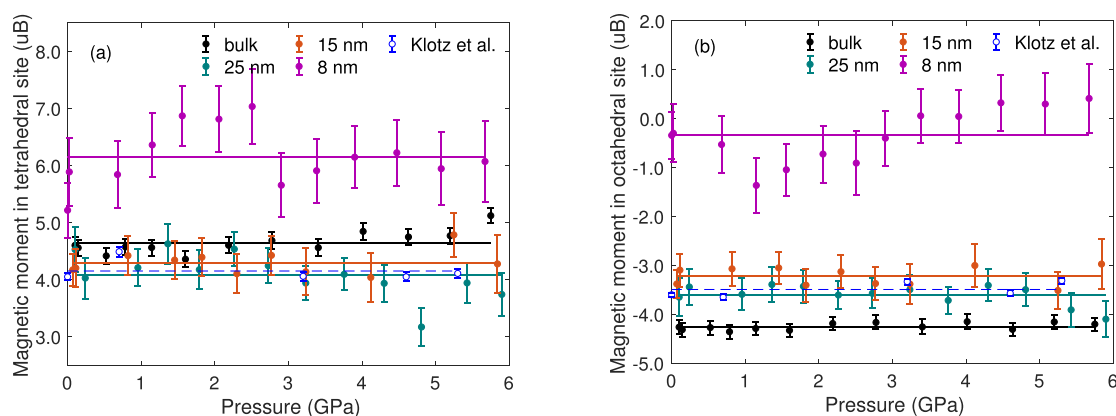


FIG. 5. The refined values of the magnetic moments in the tetrahedral (a) and octahedral (b) sites as a function of pressure of Fe_3O_4 bulk and Fe_3O_4 nanoparticles in three different sizes 25, 15, and 8 nm. The fitted straight lines are guide to the eye. The blue open circles and dashed line are from the previous neutron diffraction results on the Fe_3O_4 bulk phase reported by Klotz *et al.*³² (a) Tetrahedral magnetic moment and (b) octahedral magnetic moment.

similar to that observed in the bond length as discussed above. The magnetic moment on the tetrahedral site is larger (positive values) and on the octahedral site is less negative compared with the other two samples in different sizes. It is known that there is a spin canting effect for the small magnetite nanoparticles; the ions in the surface layer are inclined at various angles to the direction of the net moment, which caused a decrease in magnetization.^{43–45} The degree of spin canting increases with decreasing particle size. Because of this, the iron oxide nanoparticles can be regarded as core/shell structures composed of a magnetic core and a magnetically disordered shell.^{12,46} Thus, when the particle size gets smaller, the shell of the nanoparticles becomes more prominent and disordered. This is a possible explanation for the remarkable difference in magnetic moments for the 8 nm sample.

It is reported that for the 7 nm Fe_2O_3 nanoparticle, which also has a spin canted surface, the thickness of the spin canted surface layer of magnetite is deduced to be 0.9 nm.⁴³ If we assume the thickness of the canting layer is 0.9 nm for all the nanoparticles, the fraction of the scanted layer in the sample is 20% for the 25 nm sample, 32% of spins are canted for 15 nm, whereas more than half of spins (53%) are canted for the 8 nm sample. Thus, the disordered shell becomes more prominent in this sample, which may explain the substantial change in the magnetic moments of tetrahedral and octahedral sites of the 8 nm sample.

In summary, we have presented the results from a high-pressure neutron powder diffraction study of the atomic and magnetic structures of Fe_3O_4 nanoparticles under varying pressure. It is known that the particle size may influence the compressibility of nanoparticles; however, in the case of magnetite nanoparticles, it gets softer with the decrease in size. We also showed that the lattice parameters decreased with decreasing size, which is in contrast to the lattice expansion with decreasing size observed in other metal oxides.³⁴ Both the tetrahedral and octahedral bond lengths show a pressure independent trend that does not show a large variation with particle size. However, it was found that there are significant changes in the structure and magnetic properties of the smallest nanoparticle. It can be attributed to a change in the structure from the inverse to disordered spinel and also in the magnetically disordered shell that arises from the surface

disorder in magnetite nanoparticles. The synchrotron x ray total scattering technique and PDF calculation were adapted to confirm the interpretation.

Neutron powder diffraction measurements are necessarily slow compared to measurements with synchrotron radiation, and, therefore, the scope for a suite of samples is very limited in a study such as ours. Our choice of neutron diffraction was motivated by our desire to measure not only the atomic structure but also the magnetic structure. We consider that it would be worth performing new measurements with synchrotron radiation with a wider range of particle sizes than was possible in this study.

See the [supplementary material](#) for a brief introduction to the sample synthesis, all the data from Rietveld refinement, and a detailed discussion on the x-ray total scattering studies.

H.L. thanks the National Key R&D Program of China (No. 2017YFA0403801) and the National Natural Science Foundation of China (No. U1732120) for financial support. This work was also financially supported by the National Natural Science Foundation of China (No. 41874103). We gratefully acknowledge the Science and Technology Facilities Council (STFC) for access to neutron beamline PEARL at ISIS (Proposal No. RB1810556).

AUTHOR DECLARATIONS

Conflict of Interest

The authors have no conflicts to disclose.

DATA AVAILABILITY

The data that support the findings of this study are openly available in STFC ISIS Facility at <https://doi.org/10.5286/ISIS.E.RB1810556>, Ref. 47.

REFERENCES

1. Ju, T.-Y. Cai, H.-S. Lu, and C.-D. Gong, "Pressure-induced crystal structure and spin-state transitions in magnetite (Fe_3O_4)," *J. Am. Chem. Soc.* **134**, 13780–13786 (2012).

- ²L. S. Dubrovinsky, N. A. Dubrovinskaya, C. McCammon, G. K. Rozenberg, R. Ahuja, J. M. Osorio-Guillen, V. Dmitriev, H. P. Weber, T. Le Bihan, and B. Johansson, "The structure of the metallic high-pressure Fe_3O_4 polymorph: Experimental and theoretical study," *J. Phys.: Condens. Matter* **15**, 7697 (2003).
- ³W. M. Xu, G. Y. Machavariani, G. K. Rozenberg, and M. P. Pasternak, "Mössbauer and resistivity studies of the magnetic and electronic properties of the high-pressure phase of Fe_3O_4 ," *Phys. Rev. B* **70**, 174106 (2004).
- ⁴G. K. Rozenberg, Y. Amiel, W. M. Xu, M. P. Pasternak, R. Jeanloz, M. Hanfland, and R. D. Taylor, "Structural characterization of temperature- and pressure-induced inverse \leftrightarrow normal spinel transformation in magnetite," *Phys. Rev. B* **75**, 020102 (2007).
- ⁵Y. Ding, D. Haskel, S. G. Ovchinnikov, Y.-C. Tseng, Y. S. Orlov, J. C. Lang, and H.-K. Mao, "Novel pressure-induced magnetic transition in magnetite (Fe_3O_4)," *Phys. Rev. Lett.* **100**, 045508 (2008).
- ⁶K. Glazyrin, C. McCammon, L. Dubrovinsky, M. Merlini, K. Schollenbruch, A. Woodland, and M. Hanfland, "Effect of high pressure on the crystal structure and electronic properties of magnetite below 25 GPa," *Am. Mineral.* **97**, 128–133 (2012).
- ⁷A. L.-T. Pham, C. Lee, F. M. Doyle, and D. L. Sedlak, "A silica-supported iron oxide catalyst capable of activating hydrogen peroxide at neutral pH values," *Environ. Sci. Technol.* **43**, 8930–8935 (2009).
- ⁸I. C. Lekshmi, R. Buonsanti, C. Nobile, R. Rinaldi, P. D. Cozzoli, and G. Maruccio, "Tunneling magnetoresistance with sign inversion in junctions based on iron oxide nanocrystal superlattices," *ACS Nano* **5**, 1731–1738 (2011).
- ⁹G. Singh, H. Chan, A. Baskin, E. Gelman, N. Repnin, P. Král, and R. Klajn, "Self-assembly of magnetite nanocubes into helical superstructures," *Science* **345**, 1149–1153 (2014).
- ¹⁰S. ichi Ohkoshi, A. Namai, M. Yoshikiyo, K. Imoto, K. Tamazaki, K. Matsuno, O. Inoue, T. Ide, K. Masada, M. Goto, T. Goto, T. Yoshida, and T. Miyazaki, "Multimetal-substituted epsilon-iron oxide $\epsilon\text{-Ga}_{0.31}\text{Ti}_{0.05}\text{Co}_{0.05}\text{Fe}_{1.59}\text{O}_3$ for next-generation magnetic recording tape in the big-data era," *Angew. Chem.* **128**, 11575–11578 (2016).
- ¹¹H. Wang, T. Zhu, K. Zhao, W. Wang, C. Wang, Y. Wang, and W. Zhan, "Surface spin glass and exchange bias in Fe_3O_4 nanoparticles compacted under high pressure," *Phys. Rev. B* **70**, 092409 (2004).
- ¹²A. Mitra, J. Mohapatra, S. S. Meena, C. V. Tomy, and M. Aslam, "Verwey transition in ultrasmall-sized octahedral Fe_3O_4 nanoparticles," *J. Phys. Chem. C* **118**, 19356–19362 (2014).
- ¹³S. Ferrari, R. S. Kumar, F. Grinblat, J. C. Apesteguy, F. D. Saccone, and D. Errandonea, "In-situ high-pressure x-ray diffraction study of zinc ferrite nanoparticles," *Solid State Sci.* **56**, 68–72 (2016).
- ¹⁴S. Disch, E. Wetterskog, R. P. Hermann, A. Wiedenmann, U. Vainio, G. Salazar-Alvarez, L. Bergström, and T. Brückel, "Quantitative spatial magnetization distribution in iron oxide nanocubes and nanospheres by polarized small-angle neutron scattering," *New J. Phys.* **14**, 013025 (2012).
- ¹⁵R. S. DiPietro, H. G. Johnson, S. P. Bennett, T. J. Nummy, L. H. Lewis, and D. Heiman, "Determining magnetic nanoparticle size distributions from thermomagnetic measurements," *Appl. Phys. Lett.* **96**, 222506 (2010).
- ¹⁶B. H. Kim, K. Shin, S. G. Kwon, Y. Jang, H.-S. Lee, H. Lee, S. W. Jun, J. Lee, S. Y. Han, Y.-H. Yim, D.-H. Kim, and T. Hyeon, "Sizing by weighing: Characterizing sizes of ultrasmall-sized iron oxide nanocrystals using MALDI-TOF mass spectrometry," *J. Am. Chem. Soc.* **135**, 2407–2410 (2013).
- ¹⁷N. Su, Y. Han, Y. Ma, H. Liu, B. Ma, and C. Gao, "Pressure-induced magnetoresistivity reversal in magnetite," *Appl. Phys. Lett.* **99**, 211902 (2011).
- ¹⁸J. Jiang, J. S. Olsen, L. Gerward, and S. Mørup, "Enhanced bulk modulus and reduced transition pressure in $\gamma\text{-Fe}_2\text{O}_3$ nanocrystals," *Europhys. Lett.* **44**, 620 (1998).
- ¹⁹Z. Wang, Y. Zhao, D. Schiferl, J. Qian, R. T. Downs, H.-K. Mao, and T. Sekine, "Threshold pressure for disappearance of size-induced effect in spinel-structure Ge_3N_4 nanocrystals," *J. Phys. Chem. B* **107**, 14151–14153 (2003).
- ²⁰B. Palosz, S. Stel'makh, E. Grzanka, S. Gierlotka, R. Pielaszek, U. Bismayer, S. Werner, and W. Palosz, "High pressure x-ray diffraction studies on nanocrystalline materials," *J. Phys.: Condens. Matter* **16**, S353–S377 (2004).
- ²¹Q. Gu, G. Krauss, W. Steurer, F. Gramm, and A. Cervellino, "Unexpected high stiffness of Ag and Au nanoparticles," *Phys. Rev. Lett.* **100**, 045502 (2008).
- ²²M. Greuer, J. Markmann, R. Karos, W. Arnold, and R. Birringer, "Shear softening of grain boundaries in nanocrystalline Pd," *Acta Mater.* **59**, 1523–1529 (2011).
- ²³S. H. Tolbert and A. Alivisatos, "The wurtzite to rock salt structural transformation in CdSe nanocrystals under high pressure," *J. Chem. Phys.* **102**, 4642–4656 (1995).
- ²⁴Z. Wang, L. L. Daemen, Y. Zhao, C. Zha, R. T. Downs, X. Wang, Z. L. Wang, and R. J. Hemley, "Morphology-tuned wurtzite-type ZnS nanobelts," *Nat. Mater.* **4**, 922–927 (2005).
- ²⁵A. Mikhaykin, V. Dmitriev, S. Chagovets, A. Kuriganova, N. Smirnova, and I. Leontyev, "The compressibility of nanocrystalline Pt," *Appl. Phys. Lett.* **101**, 173111 (2012).
- ²⁶S. Ferrari, V. Bilovol, L. G. Pampillo, F. Grinblat, and D. Errandonea, "High pressure in-situ X-ray diffraction study on Zn-doped magnetite nanoparticles," *Solid State Sci.* **77**, 1–4 (2018).
- ²⁷S. J. L. Billinge and I. Levin, "The problem with determining atomic structure at the nanoscale," *Science* **316**, 561–565 (2007).
- ²⁸M. S. Senn, J. P. Wright, and J. P. Attfield, "Charge order and three-site distortions in the Verwey structure of magnetite," *Nature* **481**, 173–176 (2012).
- ²⁹G. Perversi, J. Cumby, E. Pachoud, J. P. Wright, and J. Attfield, "The Verwey structure of a natural magnetite," *Chem. Commun.* **52**, 4864–4867 (2016).
- ³⁰A. Patterson, "The Scherrer formula for x-ray particle size determination," *Phys. Rev.* **56**, 978 (1939).
- ³¹J. W. G. Thomason, "The ISIS spallation neutron and muon source: The first thirty-three years," *Nucl. Instrum. Methods Phys. Res., Sect. A* **917**, 61–67 (2019).
- ³²S. Klotz, G. Rousse, T. Strässle, C. L. Bull, and M. Guthrie, "Nuclear and magnetic structure of magnetite under pressure to 5.3 GPa and at low temperatures to 130 K by neutron scattering," *Phys. Rev. B* **74**, 012410 (2006).
- ³³C. Mays, J. Vermaak, and D. Kuhlmann-Wilsdorf, "On surface stress and surface tension," *Surf. Sci.* **12**, 134–140 (1968).
- ³⁴P. M. Diehm, P. Ágoston, and K. Albe, "Size-dependent lattice expansion in nanoparticles: Reality or anomaly?," *ChemPhysChem* **13**, 2443–2454 (2012).
- ³⁵P. P. Rodenbough, J. Song, D. Walker, S. M. Clark, B. Kalkan, and S.-W. Chan, "Size dependent compressibility of nano-ceria: Minimum near 33 nm," *Appl. Phys. Lett.* **106**, 163101 (2015).
- ³⁶D. Prieur, W. Bonani, K. Popa, O. Walter, K. W. Kriegsman, M. H. Engelhard, X. Guo, R. Eloirdi, T. Gouder, A. Beck, T. Vitova, A. C. Scheinost, K. Kvashnina, and P. Martin, "Size dependence of lattice parameter and electronic structure in CeO_2 nanoparticles," *Inorg. Chem.* **59**, 5760–5767 (2020).
- ³⁷J. S. Vermaak, C. W. Mays, and D. Kuhlmann-Wilsdorf, "On surface stress and surface tension," *Surf. Sci.* **12**, 128–133 (1968).
- ³⁸J. Weissmüller and J. W. Cahn, "Mean stresses in microstructures due to interface stresses: A generalization of a capillary equation for solids," *Acta Mater.* **45**, 1899–1906 (1997).
- ³⁹L. W. Finger, R. M. Hazen, and A. M. Hofmeister, "High-pressure crystal chemistry of spinel (MgAl_2O_4) and magnetite (Fe_3O_4): Comparisons with silicate spinels," *Phys. Chem. Miner.* **13**, 215–220 (1986).
- ⁴⁰K. Bian, W. Bassett, Z. Wang, and T. Hanrath, "The strongest particle: Size-dependent elastic strength and Debye temperature of PbS nanocrystals," *J. Phys. Chem. Lett.* **5**, 3688–3693 (2014).
- ⁴¹I. D. Brown and D. Altermatt, "Bond-valence parameters obtained from a systematic analysis of the inorganic crystal structure database," *Acta Crystallogr., Sect. B* **41**, 244–247 (1985).
- ⁴²A. Bengtson, D. Morgan, and U. Becker, "Spin state of iron in Fe_3O_4 magnetite and h- Fe_3O_4 ," *Phys. Rev. B* **87**, 155141 (2013).
- ⁴³S. Linderth, P. V. Hendriksen, F. Bødker, S. Wells, K. Davies, S. W. Charles, and S. Mørup, "On spin-canting in maghemite particles," *J. Appl. Phys.* **75**, 6583–6585 (1994).
- ⁴⁴E. Lima, A. L. Brandl, A. D. Arelaro, and G. F. Goya, "Spin disorder and magnetic anisotropy in Fe_3O_4 nanoparticles," *J. Appl. Phys.* **99**, 083908 (2006).
- ⁴⁵D. Jiles, *Introduction to Magnetism and Magnetic Materials* (CRC Press, 2015).
- ⁴⁶R. Müller, R. Hergt, S. Dutz, M. Zeisberger, and W. Gawalek, "Nanocrystalline iron oxide and Ba ferrite particles in the superparamagnetism–ferromagnetism transition range with ferrofluid applications," *J. Phys.: Condens. Matter* **18**, S2527 (2006).
- ⁴⁷M. Dove, A. Phillips, L. Tan, A. Sapelkin, C. Bull, H. Tian, and J. Liu (2018). "High-pressure structure of magnetite nanoparticles," STFC ISIS Neutron and Muon Source <https://doi.org/10.5286/ISIS.ERB1810556>.